

Supplementary Information

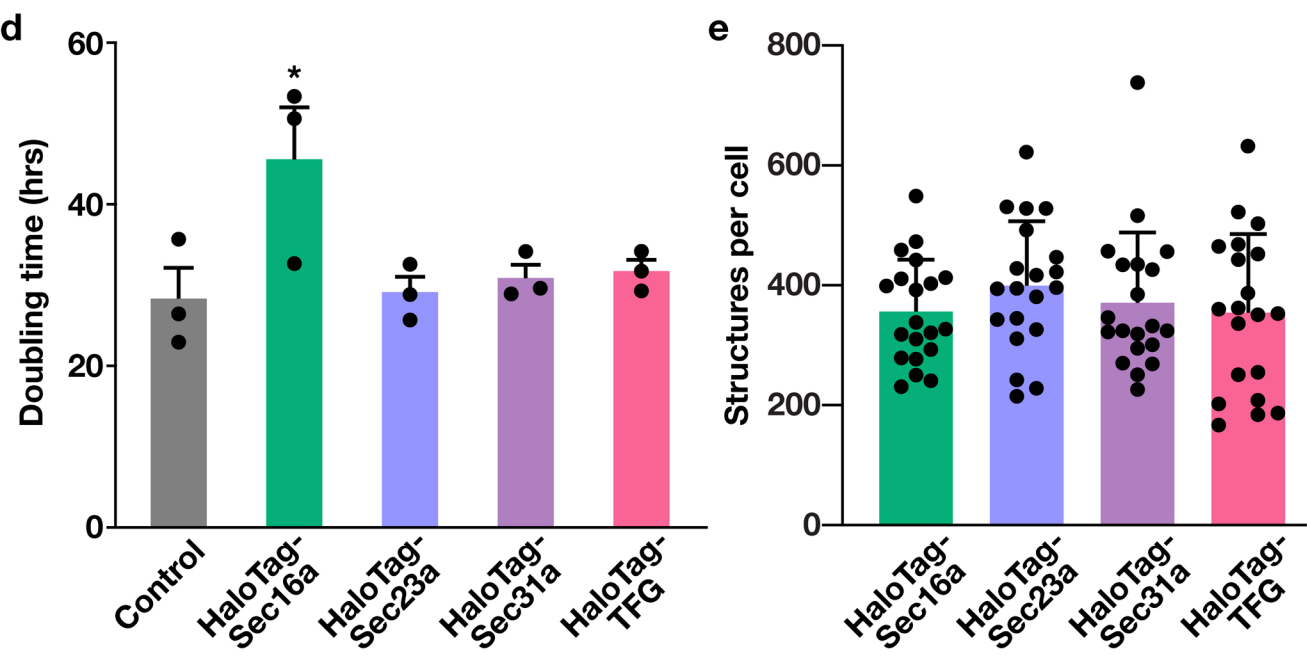
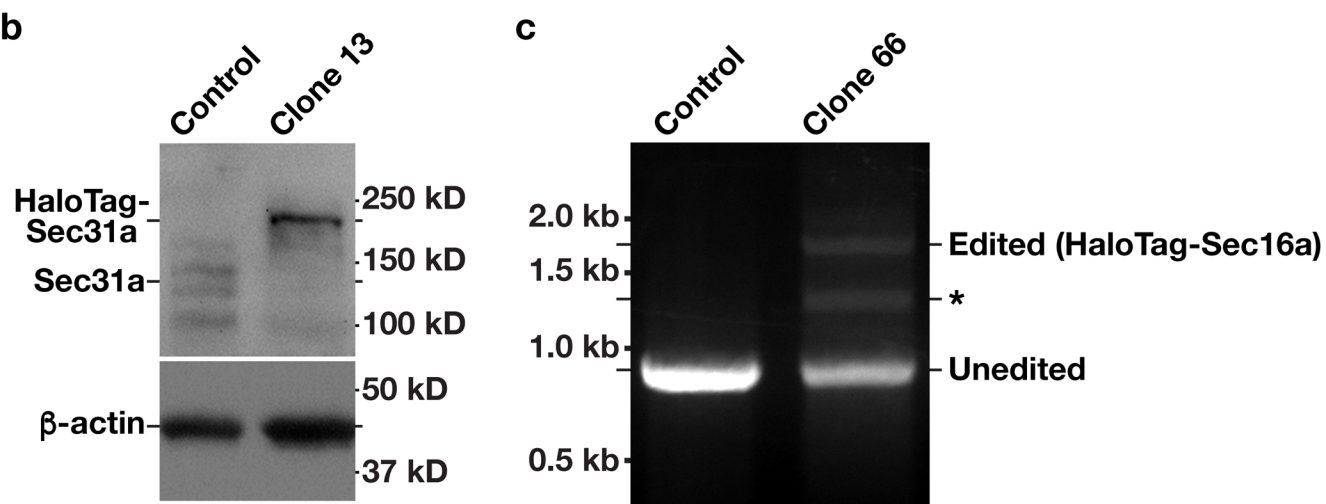
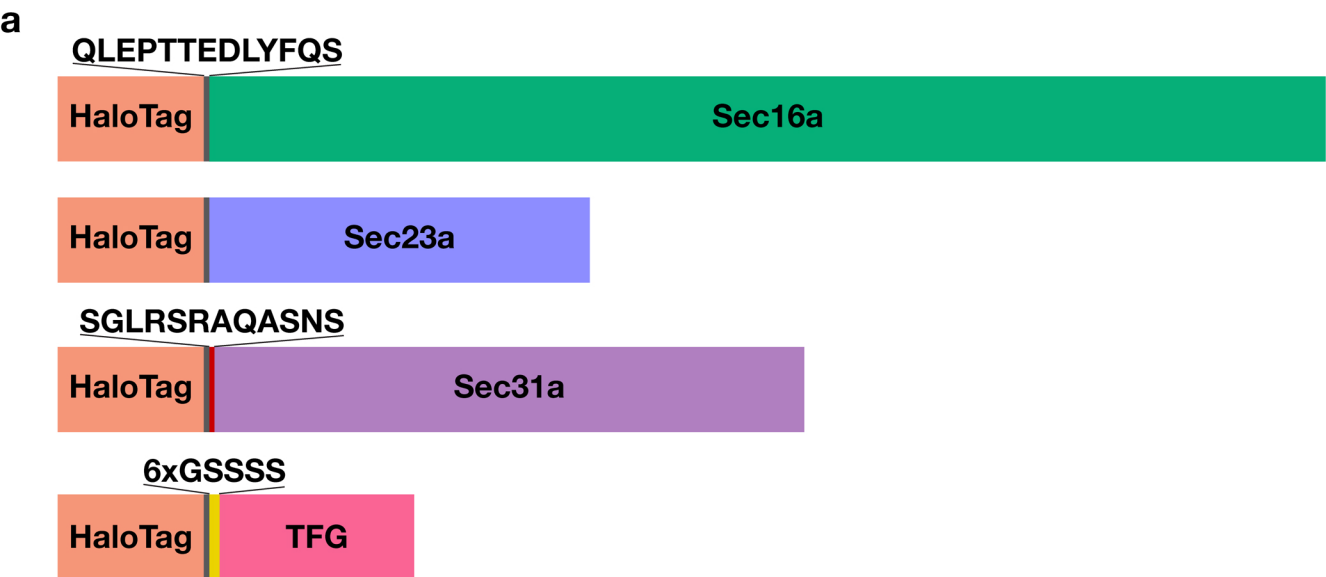


Figure S1. Appending HaloTag onto endogenous COPII subunits fails to impact their function. (A) Cartoons depicting the strategy used to create HaloTag (orange) fusions with native Sec16a (green), Sec23a (light blue) (62), Sec31a (purple), and TFG (salmon). (B) Representative immunoblots (n=3) of extracts generated from control and clonal CRISPR/Cas9 edited cell lines using antibodies directed against Sec31a (top) and β -actin (bottom). (C) PCR was used to analyze genomic DNA from control cells and clonal cells expressing a HaloTag fusion to Sec16a (n=3). An asterisk highlights a nonspecific band, based on sequence analysis. (D) The proliferation rates of control cells (grey) and genome edited cells expressing HaloTag fusion proteins (HaloTag-Sec16a, green; HaloTag-Sec23a, light blue; HaloTag-Sec31a, purple; HaloTag-TFG, salmon) were determined using widefield imaging of Calcein AM, which marks living cells. Error bars represent the mean \pm SEM (n=3 biological replicates each). *, p = 0.0315 as calculated using a one-way ANOVA and Tukey post hoc test. (E) Based on confocal microscopy, the total number of structures decorated by each HaloTag fusion protein (HaloTag-Sec16a, green; HaloTag-Sec23a, light blue; HaloTag-Sec31a, purple; HaloTag-TFG, salmon) following labeling with JFX650-HaloTag ligand was calculated throughout the volume of cells (n=20 cells each; 3 biological replicates each). No statistically significant differences were found, as calculated using a one-way ANOVA and Tukey post hoc test.

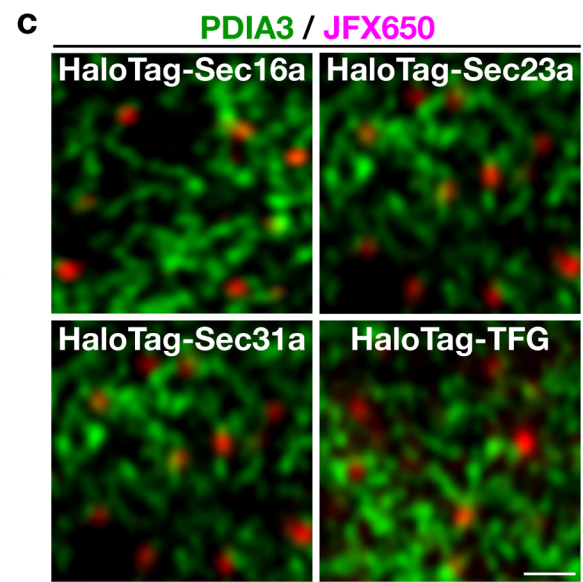
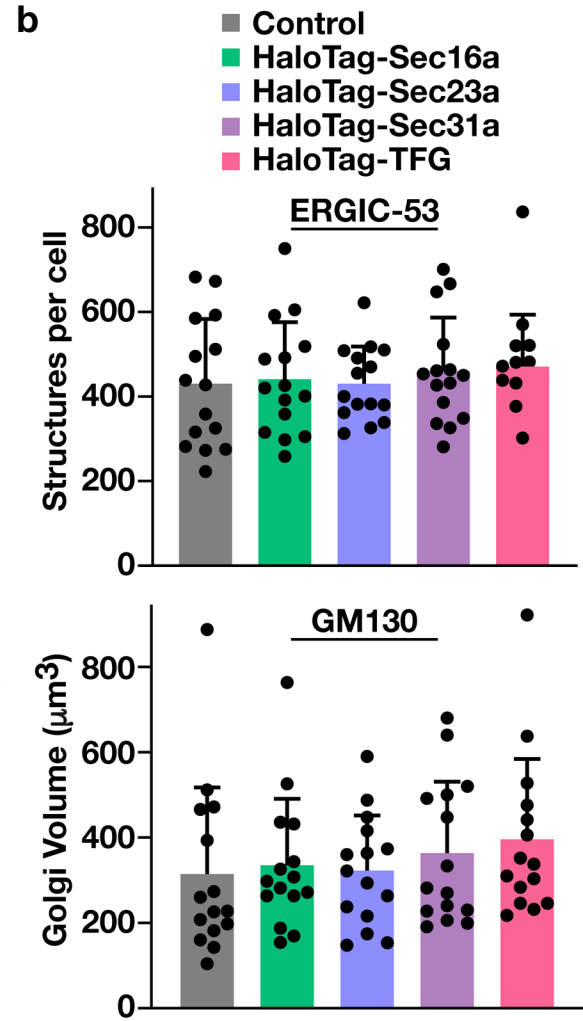
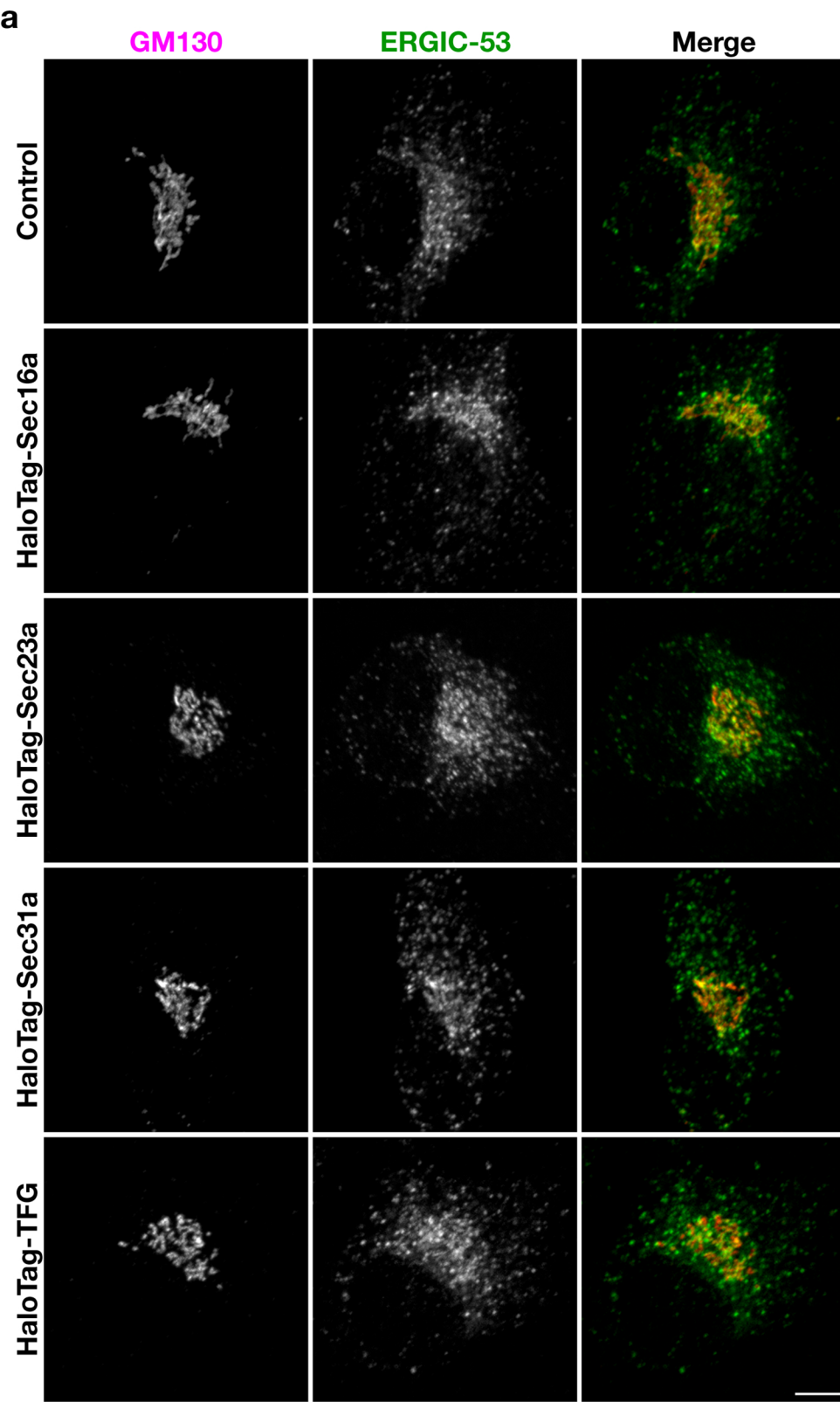


Figure S2. Genome edited cell lines exhibit normal organization of the early secretory pathway. (A) Representative confocal images of cell lines natively expressing HaloTag fusion proteins co-stained with antibodies directed against endogenous GM130 (magenta) and ERGIC-53 (green). Bar, 10 μm . (B) Based on confocal microscopy, the total number of structures decorated by ERGIC-53 (top) and the total cellular volume labeled by GM130 (bottom) was calculated within control cells (grey) and cells expressing HaloTag fusions proteins (HaloTag-Sec16a, green; HaloTag-Sec23a, light blue; HaloTag-Sec31a, purple; HaloTag-TFG, salmon) (n=15 cells each; 3 biological replicates each). No statistically significant differences were found, as calculated using a one-way ANOVA and Tukey post hoc test. (C) Representative super resolution images of fixed cells expressing HaloTag fusion proteins labeled with the JFX650-HaloTag ligand (magenta) and co-stained using antibodies directed against PDIA3 (green). Bar, 1 μm .

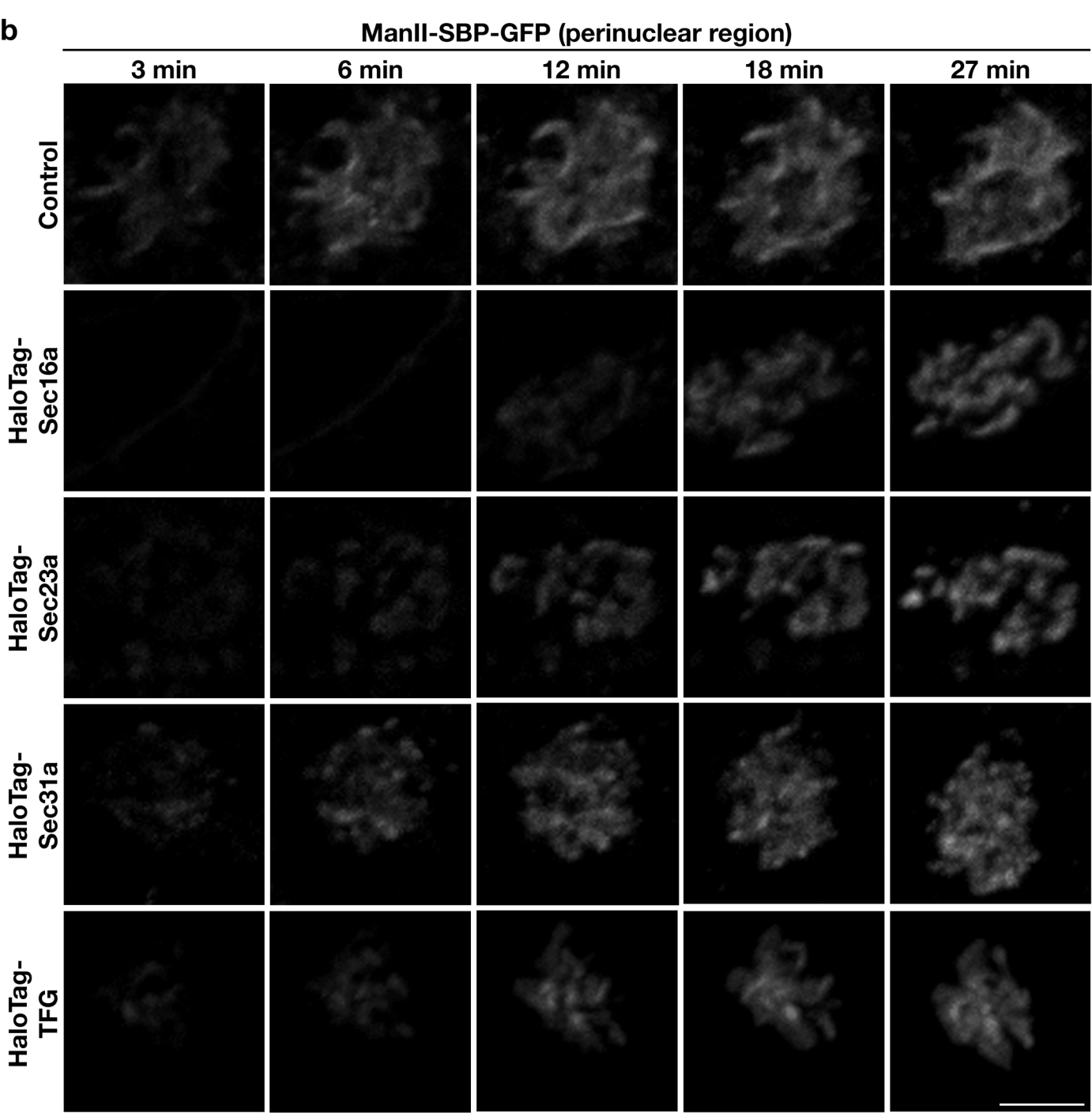
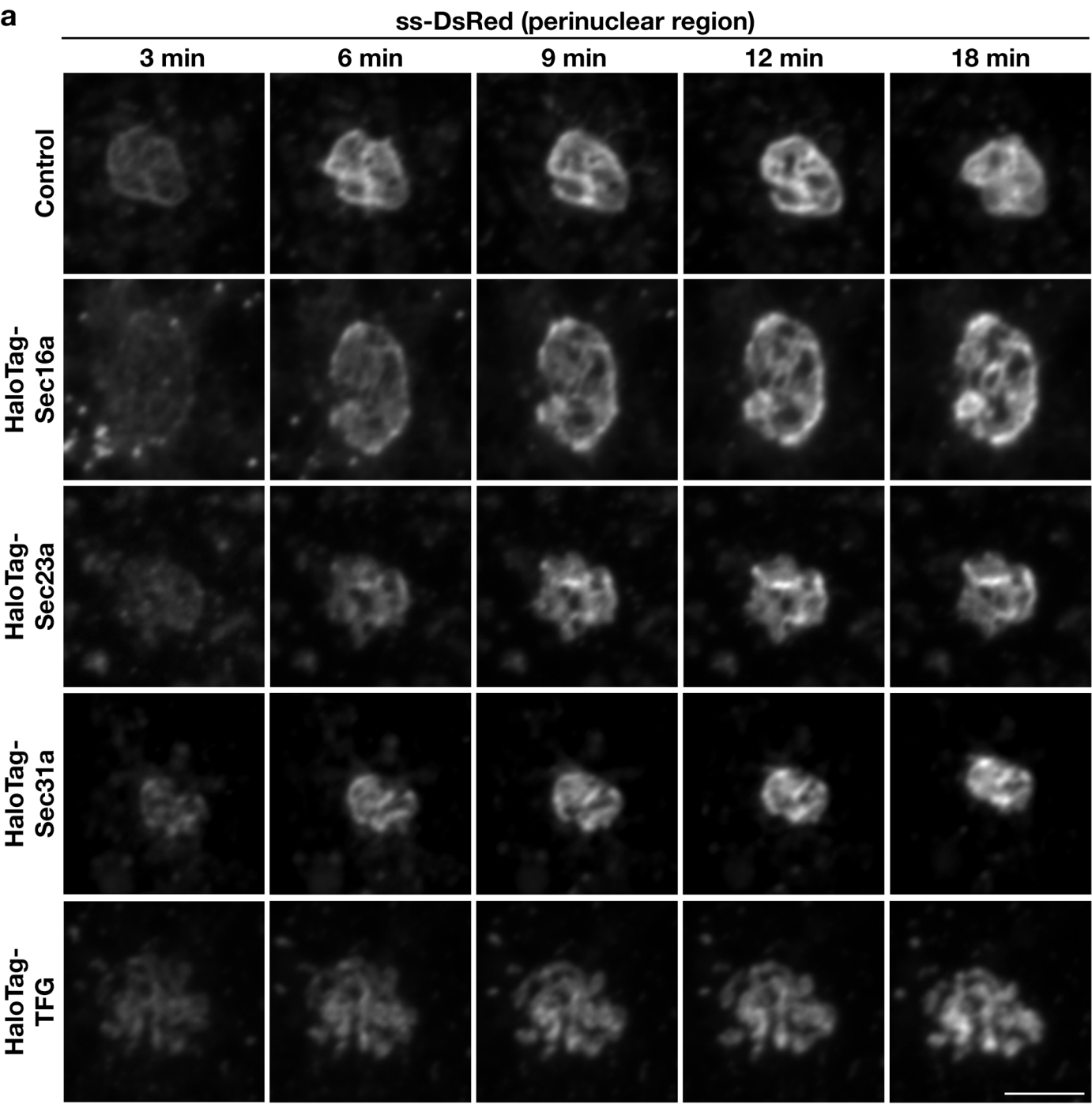


Figure S3. Genome edited cell lines exhibit normal trafficking of secretory cargoes. (A and B) Representative confocal images of control cells and cell lines natively expressing HaloTag fusion proteins co-expressing ss-DsRed (A) or ManII-SBP-GFP (B) at various timepoints following their release from the ER (n=15 cells each; 3 biological replicates each). Zoomed images of the perinuclear region are shown. Bar, 5 μ m.

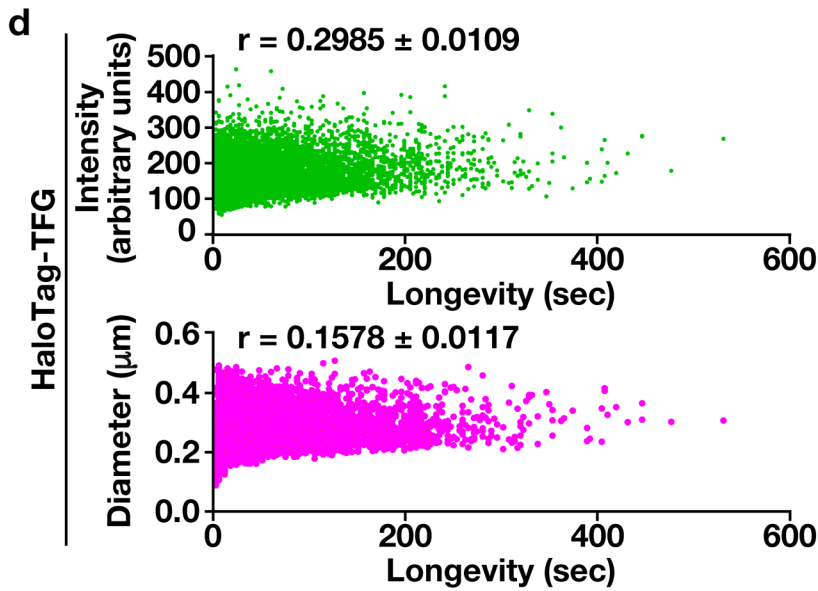
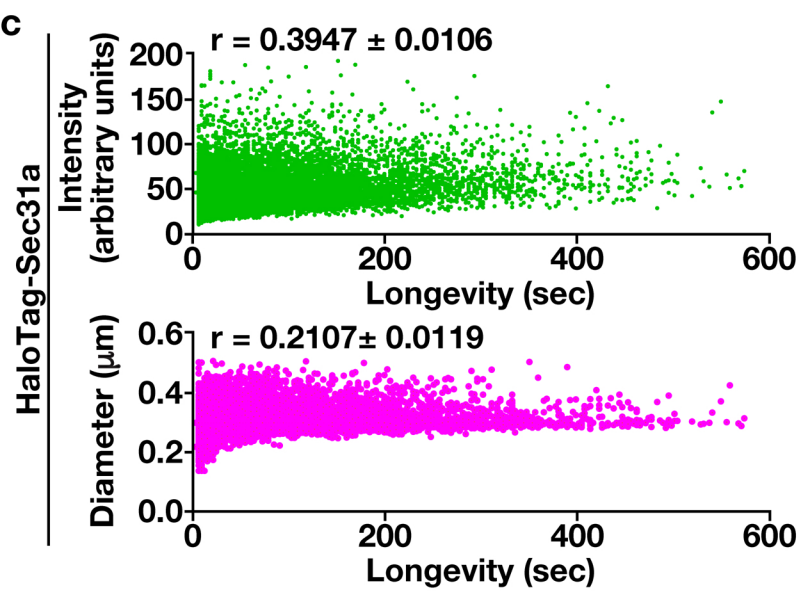
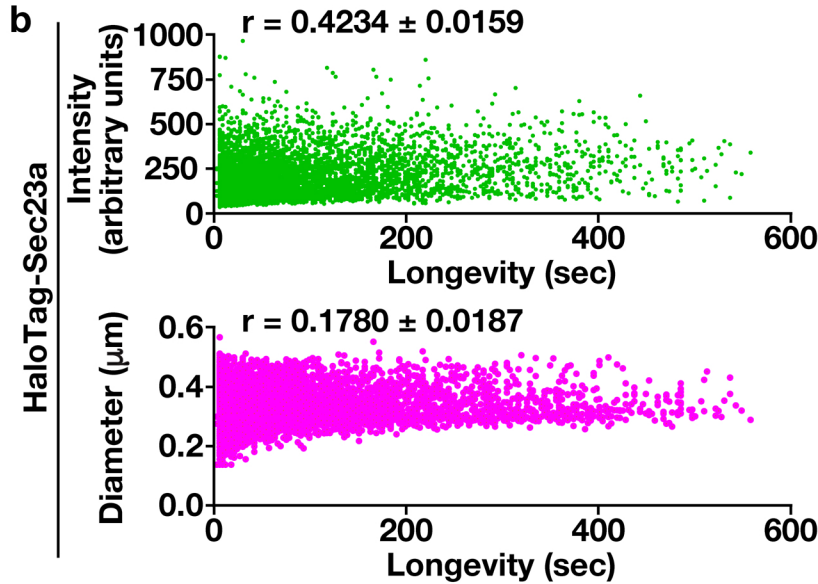
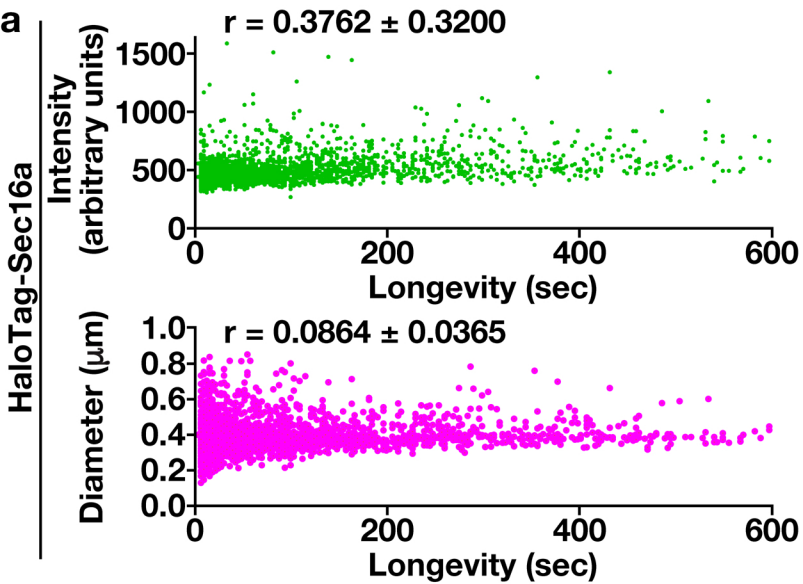


Figure S4. Long-lived structures harboring HaloTag fusion proteins exhibit increased intensity and size relative to short-lived sites. (A-D) Pearson's correlation analysis was used to calculate the covariance (represented by correlation coefficient, r) between site longevity and either intensity (top; green) or diameter (bottom; magenta) for structures harboring HaloTag fusion proteins (n=10 cells each; 3 biological replicates; more than 3000 particles each).

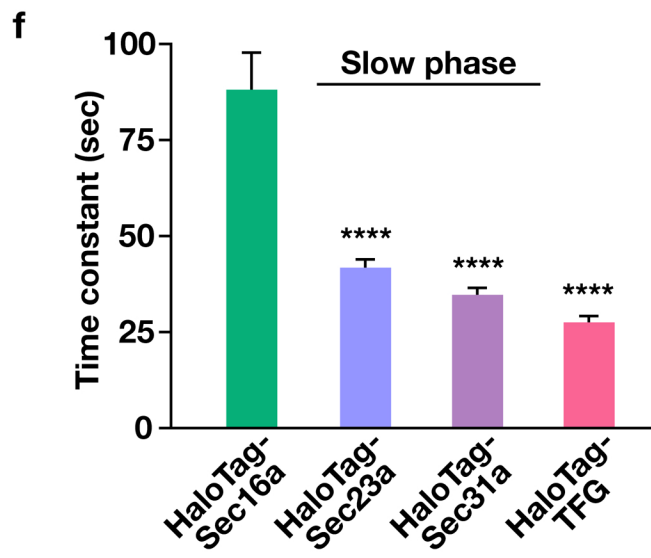
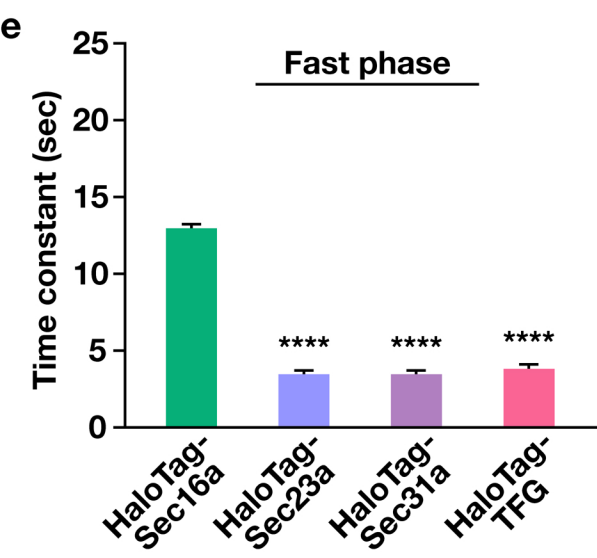
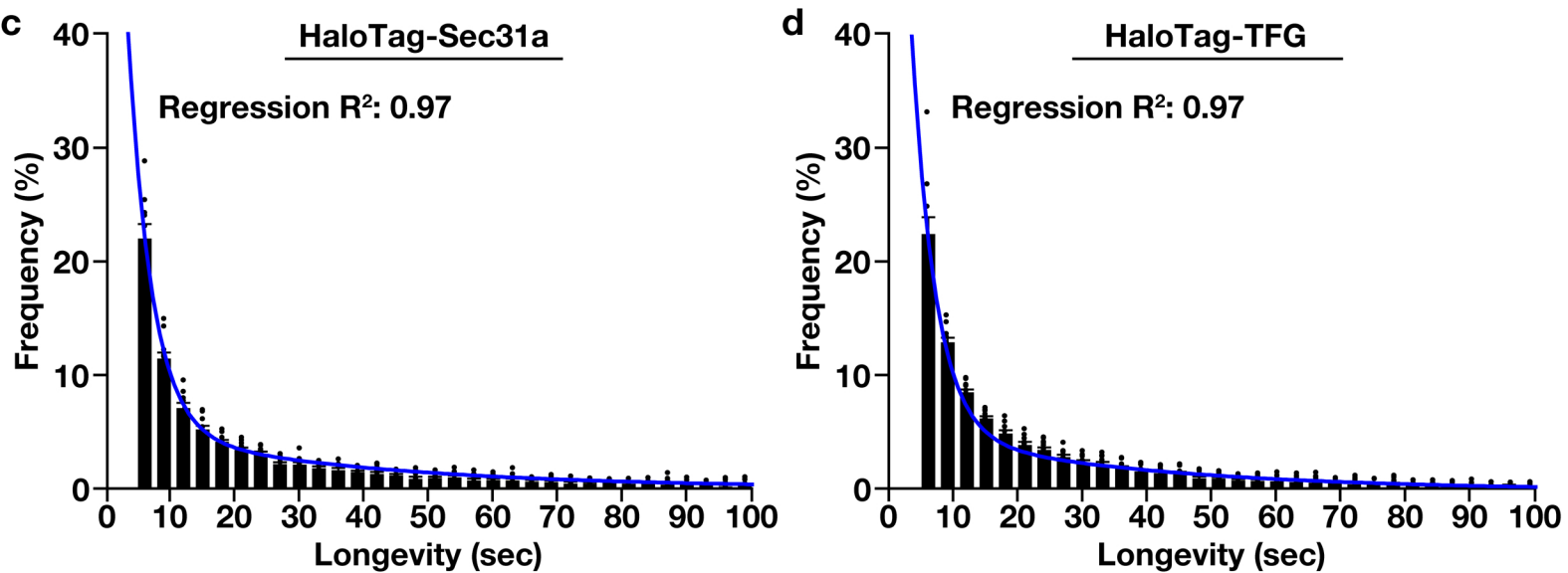
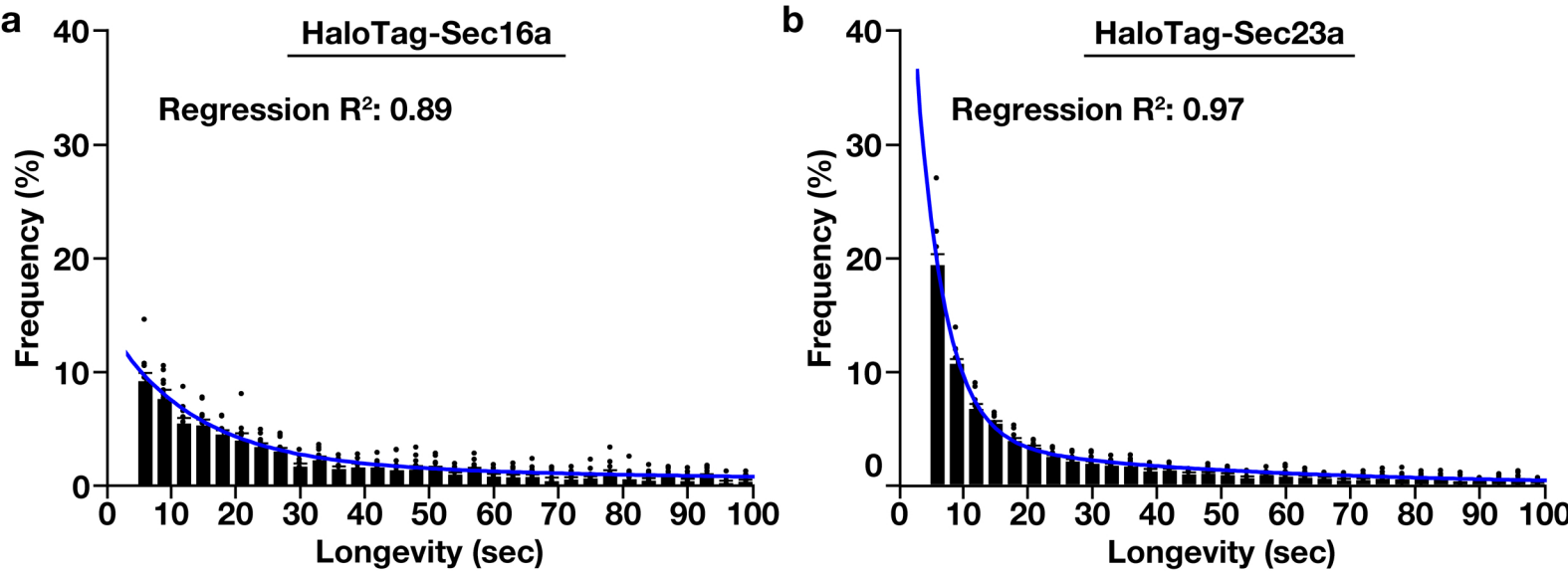


Figure S5. At least two types of sites harboring each HaloTag fusion protein are present in cells. (A-D) Based on lattice light-sheet imaging, histograms were generated to describe how frequently sites of differing longevity were found. Blue curves demonstrate fitting to a two-phase exponential decay equation (R^2 values shown). Error bars represent mean \pm SEM (n=10 cells each; 3 biological replicates; more than 3000 tracked particles each). (E and F) Based on two-phase exponential decay regressions for each HaloTag fusion protein (HaloTag-Sec16a, green; HaloTag-Sec23a, light blue; HaloTag-Sec31a, purple; HaloTag-TFG, salmon), time constants for distinct fast (E) and slow (F) phases were calculated. Error bars represent mean \pm SEM (n=10 cells each; more than 3000 structures each; 3 biological replicates). ****, $p = 0.0001$, calculated using a one-way ANOVA and Tukey post hoc test.

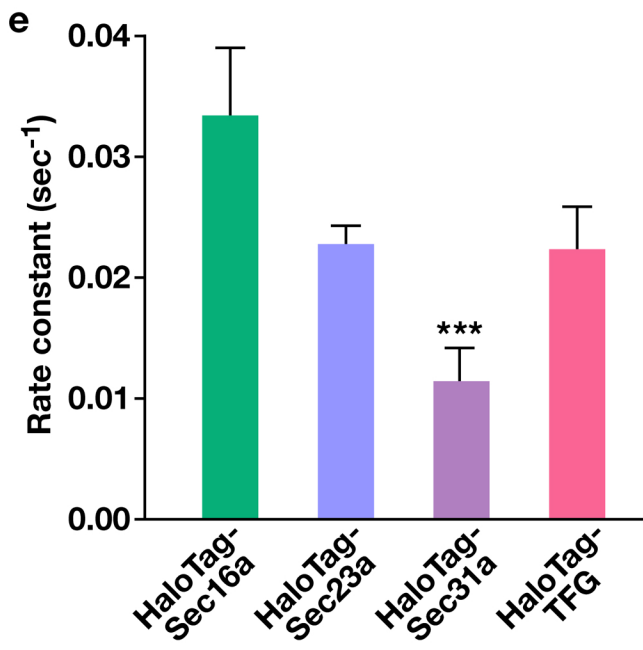
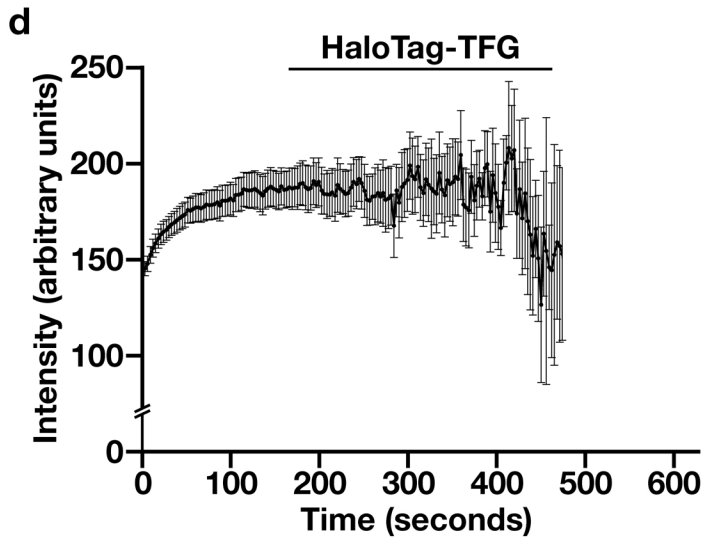
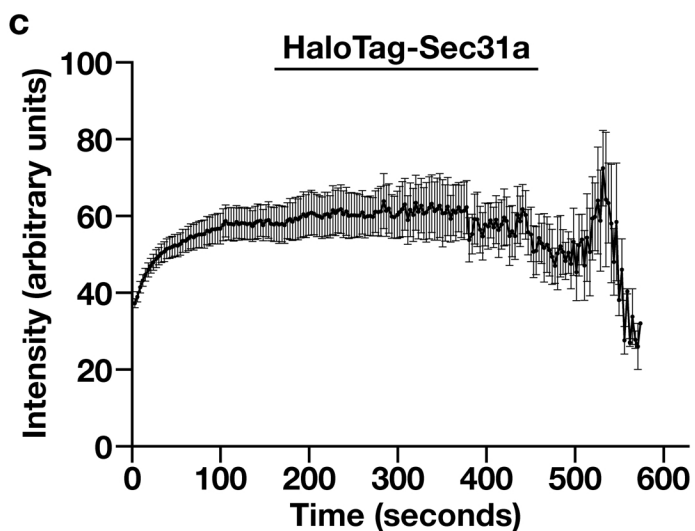
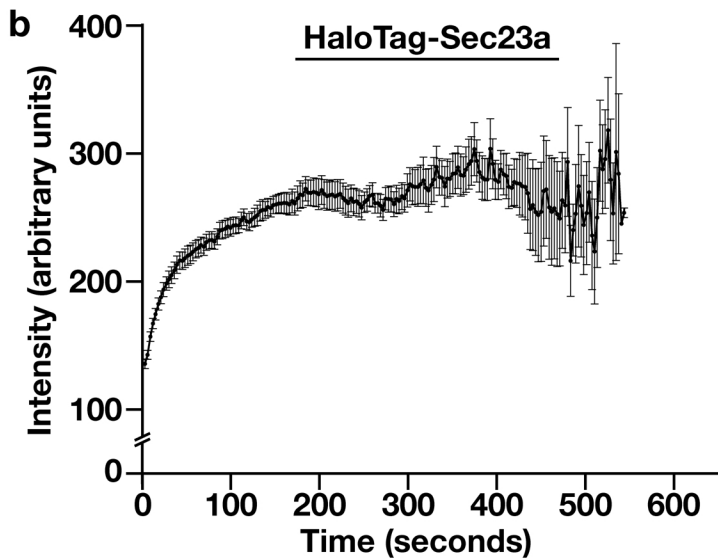
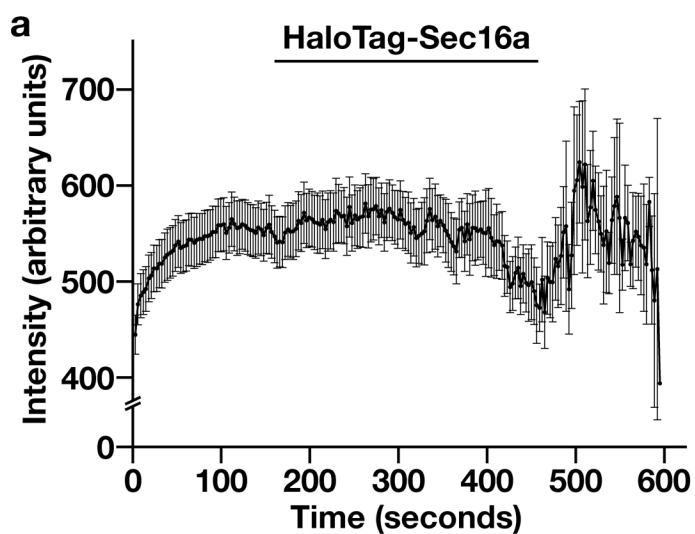


Figure S6. Dynamics of HaloTag fusion proteins at ER subdomains. (A-D) Fluorescence intensity of HaloTag-Sec16a (A), HaloTag-Sec23a (B), HaloTag-Sec31a (C), and HaloTag-TFG (D) positive structures tracked over time using light-sheet imaging following labeling with JFX650-HaloTag ligand. Error bars represent mean \pm SEM (n=10 cells each; more than 3000 structures each; 3 biological replicates). (E) Rate constants were calculated based on assembly curves for each HaloTag fusion protein (HaloTag-Sec16a, green; HaloTag-Sec23a, light blue; HaloTag-Sec31a, purple; HaloTag-TFG, salmon, fitted to an exponential plateau equation). Error bars represent mean \pm SEM (n=10 cells each; more than 3000 structures each; 3 biological replicates). ***, $p = 0.0009$, calculated using a one-way ANOVA and Tukey post hoc test.

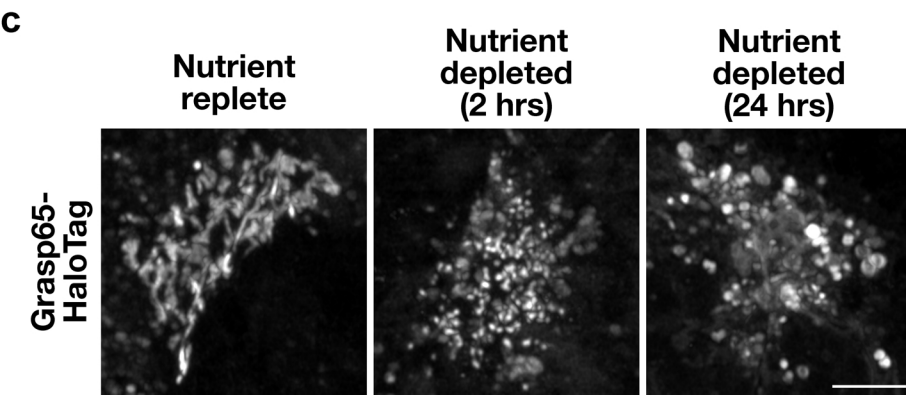
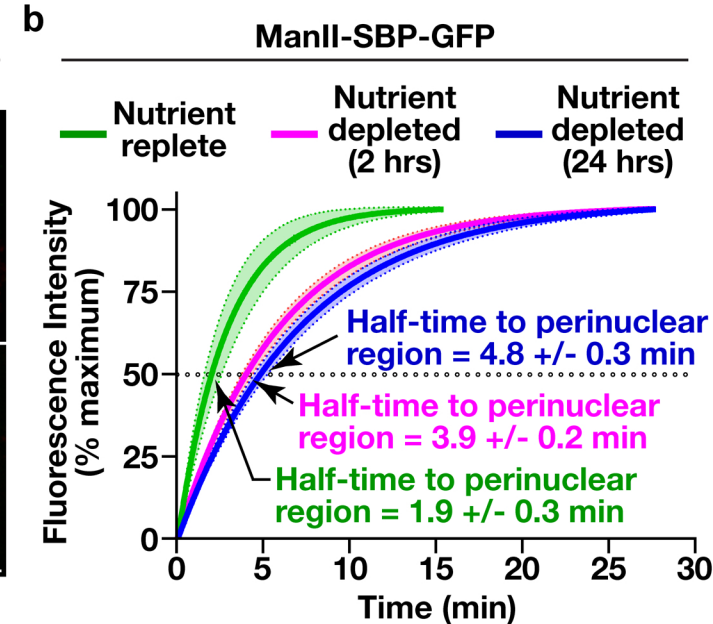
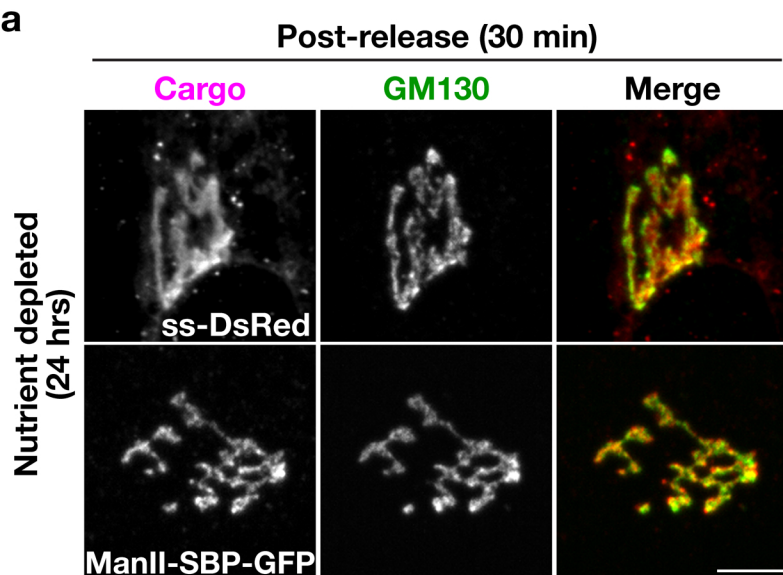


Figure S7. Acute and long-term nutrient deprivation similarly influence the rate of ManII-SBP-GFP trafficking. (A) Confocal imaging of control cells expressing ss-DsRed or ManII-SBP-GFP (magenta) was used to monitor their accumulation at Golgi membranes harboring GM130 (green) following their release from the ER under prolonged nutrient deprivation conditions. Bar, 5 μm . (B) Based on fluorescence intensity, the percentage of ManII-SBP-GFP present within the perinuclear region relative to its maximal accumulation there was quantified over time and fitted to an exponential with the dotted line indicating half-maximal intensity. Error, as displayed by lightly colored bands, represent mean \pm SEM (n=30 cells each; 3 biological replicates each). Half-times to perinuclear accumulation of ss-DsRed were calculated (see Source Data file) based on the plots under various nutrient availability conditions (nutrient replete, green; 2 hour nutrient depletion, magenta; 24 hour nutrient depletion, blue). (C) Representative super resolution images of clonal CRISPR/Cas9-edited cells expressing GRASP65-HaloTag in the presence and absence of nutrients following labeling with JFX650-HaloTag ligand. Bar, 5 μm .

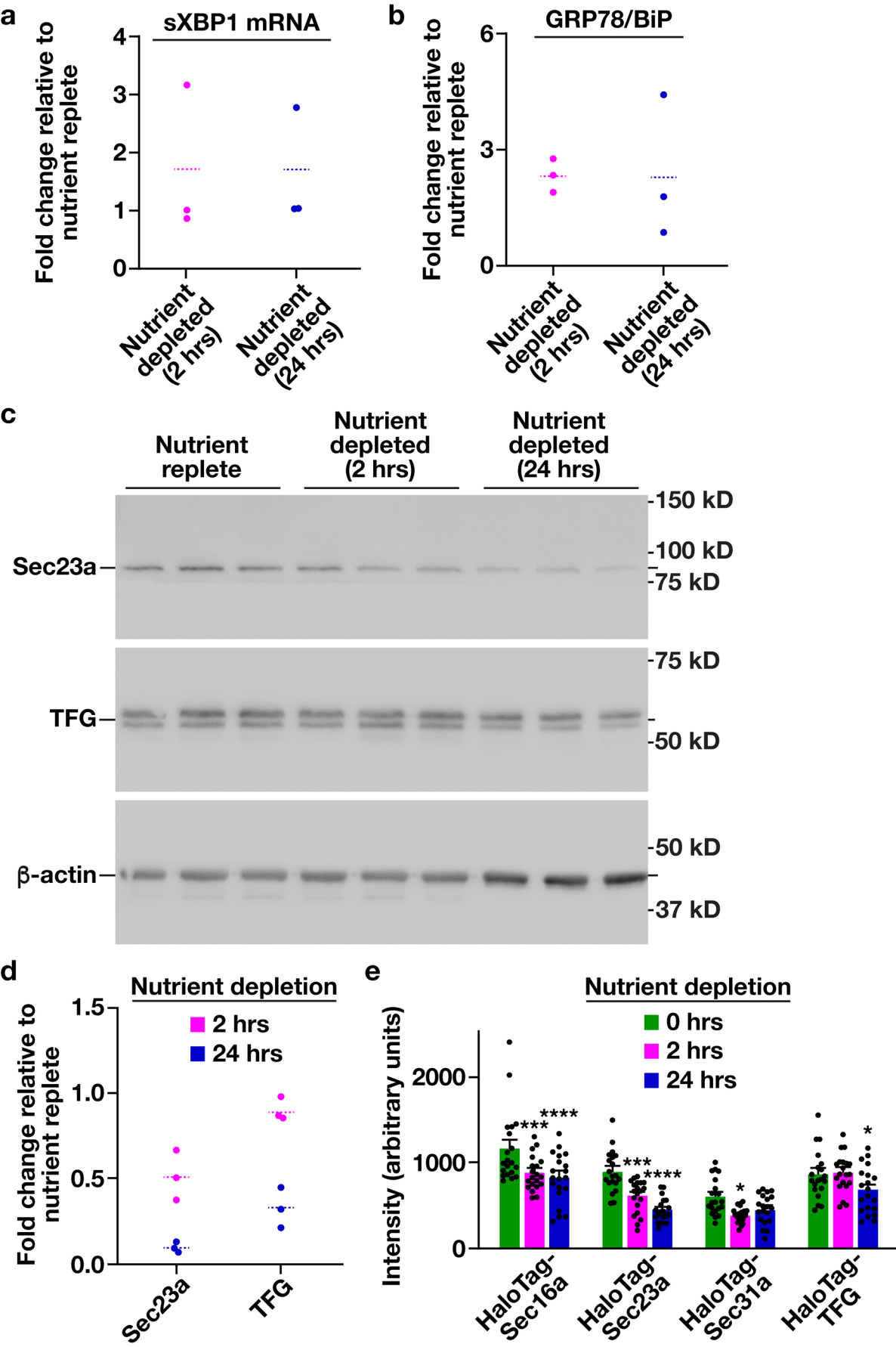


Figure S8. Nutrient deprivation reduces expression of COPII subunits. (A) Levels of sXBP1 mRNA in nutrient deprived cells were determined relative to control cells (maintained in the presence of nutrients) using quantitative PCR (2 hour nutrient depletion, magenta; 24 hour nutrient depletion, blue; n=3 biological replicates). No statistically significant differences were found, as calculated using an unpaired *t* test. (B) Levels of GRP78 in nutrient deprived cells were determined relative to control cells (maintained in the presence of nutrients) using quantitative immunoblotting (2 hour nutrient depletion, magenta; 24 hour nutrient depletion, blue; n=3 biological replicates). No statistically significant differences were found, as calculated using an unpaired *t* test. (C) Representative immunoblots (n=3 each) of extracts generated from control cells in the presence and absence of nutrients using antibodies directed against Sec23a (top), TFG (middle) and β -actin (bottom). (D) Quantification of immunoblots shown in panel C (2 hour nutrient depletion, magenta; 24 hour nutrient depletion, blue; 3 biological replicates). (E) Based on quantitative cellular fluorescence measurements, the intensity of each HaloTag fusion protein was compared in the presence and absence of nutrients (nutrient replete, green; 2 hour nutrient depletion, magenta; 24 hour nutrient depletion, blue). Error bars represent mean \pm SEM (n=20 cells each; 3 biological replicates each). *****p* = 0.001, ****p* = 0.006 (HaloTag-Sec16a nutrient replete as compared to 2 hour nutrient deprivation) or 0.005 (HaloTag-Sec23a nutrient replete as compared to 2 hour nutrient deprivation), and **p* = 0.0221 (HaloTag-Sec31a nutrient replete as compared to 2 hour nutrient deprivation) or 0.0267 (HaloTag-TFG nutrient replete as compared to 24 hour nutrient deprivation), each calculated using a one-way ANOVA and Tukey post hoc test.

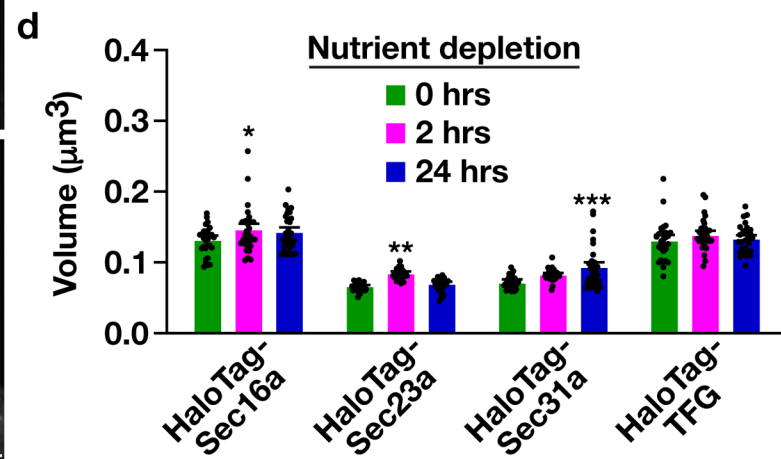
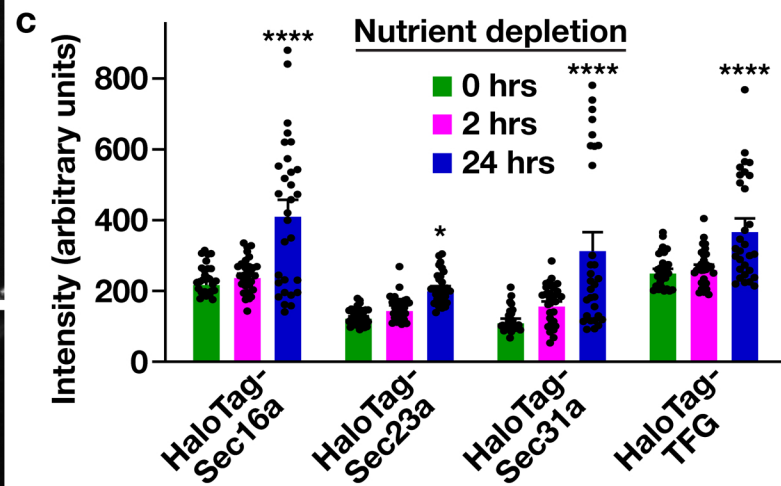
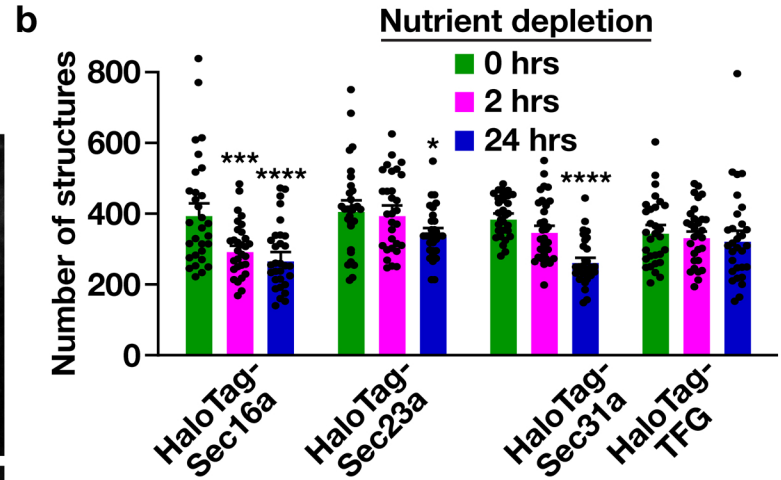
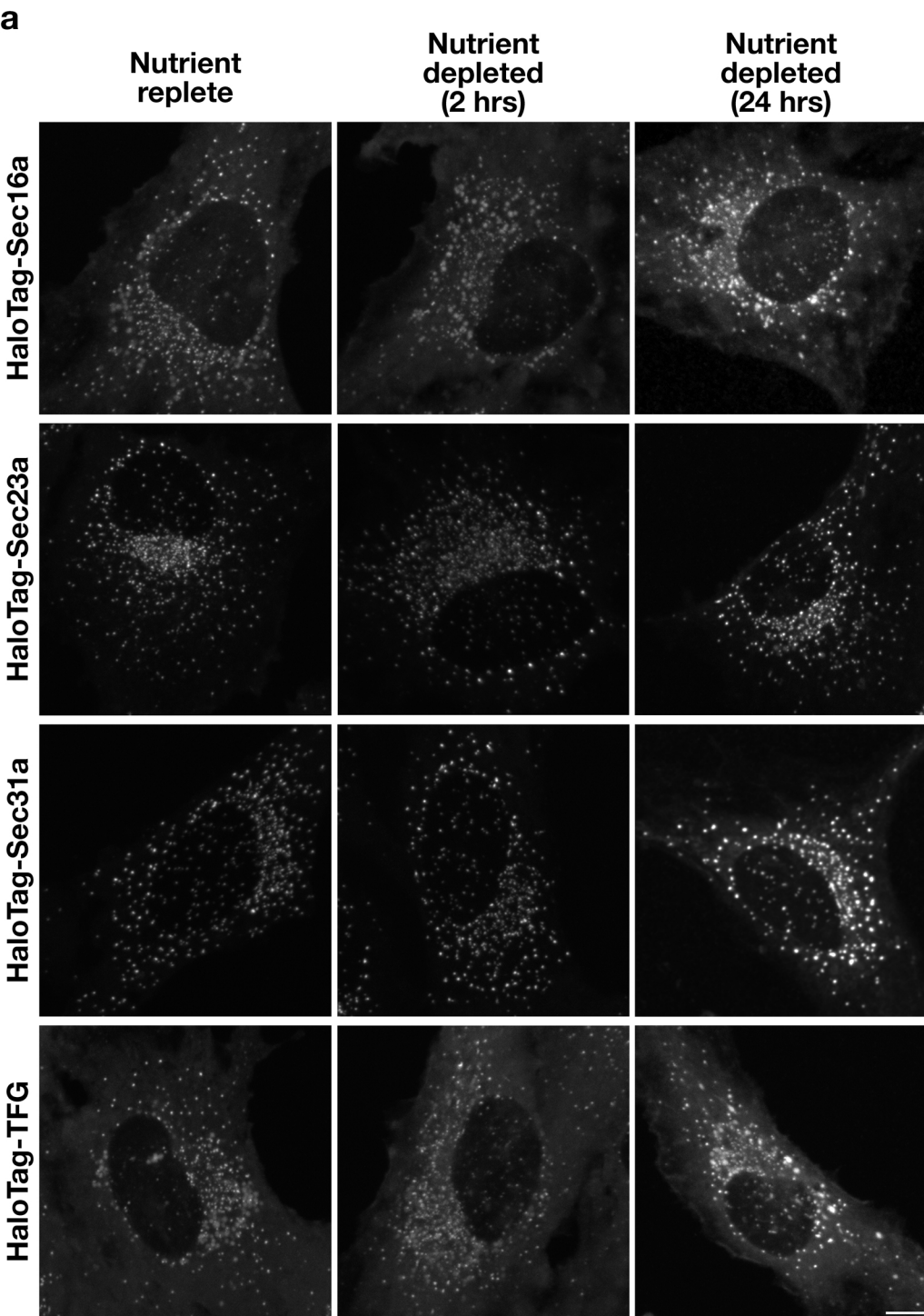


Figure S9. Long-term nutrient deprivation reduces the number of COPII-positive

structures in cells, but elevates their intensities. (A) Representative confocal images of cell lines natively expressing HaloTag fusion proteins after labeling with JFX650-HaloTag ligand in the presence and absence of nutrients are shown. Bar, 5 μm . (B-D) Based on confocal microscopy, the total number of structures decorated by each HaloTag fusion protein (B), their intensities (C) and their volumes (D) were calculated in the presence and absence of nutrients (nutrient replete, green; 2 hour nutrient depletion, magenta; 24 hour nutrient depletion, blue). Error bars represent mean \pm SEM (n=30 cells each; 3 biological replicates each). ****p = 0.0001 and *p = 0.0163 (panel B), ****p = 0.0001 and *p = 0.0116 (panel C), and ***p = 0.0003, **p = 0.0017, and *p = 0.0184 (panel D), each calculated using a one-way ANOVA and Tukey post hoc test. Additional p values for other comparisons are provided in the Source Data file.

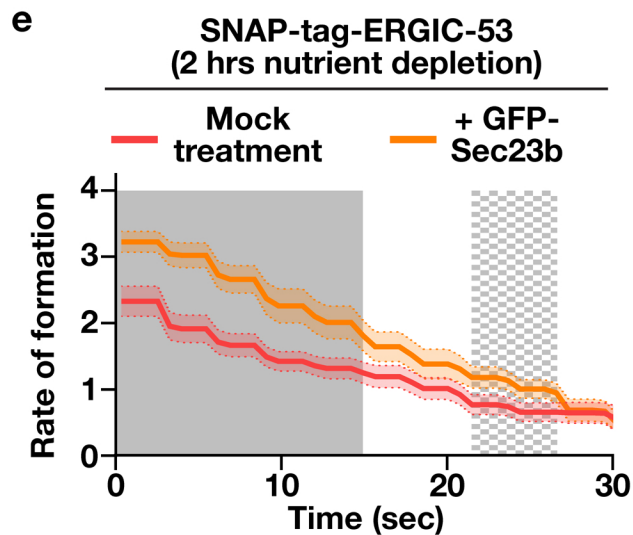
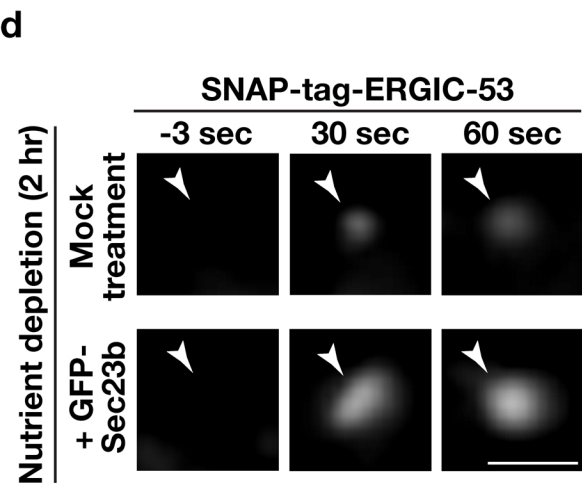
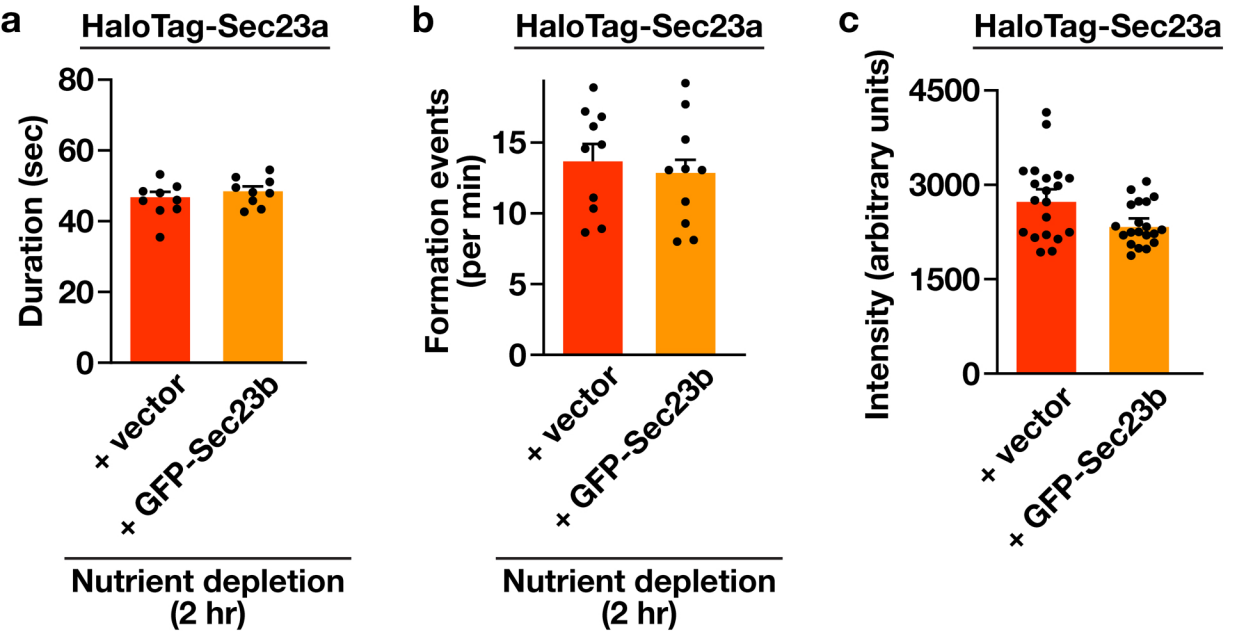


Figure S10. Overexpression of GFP-Sec23b accelerates cargo trafficking from the ER in cells depleted acutely of nutrients. (A) Quantification of the average duration of HaloTag-Sec23a at ER subdomains in the presence (yellow) or absence (orange) of overexpressed GFP-Sec23b following acute nutrient deprivation. Error bars represent mean \pm SEM (n=20 cells each; 3 biological replicates). No statistically significant difference was found, as calculated using an unpaired *t* test. (B) Quantification of the number of HaloTag-Sec23a positive structures that form each minute in the presence (yellow) or absence (orange) of overexpressed GFP-Sec23b following acute nutrient deprivation. Error bars represent mean \pm SEM (n=20 cells each; 3 biological replicates). No statistically significant differences were found, as calculated using an unpaired *t* test. (C) The total cellular intensity of HaloTag-Sec23a following labeling with JFX650-HaloTag ligand was determined in the presence (yellow) or absence (orange) of overexpressed GFP-Sec23b. Error bars represent mean \pm SEM (n=20 cells each; 3 biological replicates). No statistically significant difference was found, as calculated using an unpaired *t* test. (D) Following nutrient depletion (2 hrs), HILO imaging was used to monitor the de novo formation of sites harboring SNAP-tag-ERGIC-53 (highlighted by arrowheads) in the presence or absence of GFP-Sec23b. Bar, 1 μ m. (E) The rates at which sites harboring SNAP-tag-ERGIC-53 formed in the presence and absence of exogenously expressed GFP-Sec23b were derived from assembly curves generated from data described in panel D. Error, as displayed by lightly colored bands, represents mean \pm SEM (n=15 cells each; more than 3000 structures each; 3 biological replicates). Solid gray ($p < 0.05$) and checkered gray ($p < 0.1$) regions represent significant differences, calculated using multiple, unpaired *t* tests at each time point. Specific *p* values are provided in the Source Data file.